Algorithm Description Ver.0 (2011.09.30)
Algorithm Description Ver.0 加筆修正 (2011.10.10)
Algorithm Description Ver.1 (2014.11.12)
Algorithm Description Ver.2 (2019.3.1)

PI No. 134 Takafumi Hirata (GCOM-C/SGLI Ocean Team)

Theoretical Description of the Inherent Optical Property Algorithm

1. Derivation of the inherent optical properties (IOPs)

1.1 Physics of the problem

The IOP algorithm assumes that the remote sensing reflectance (R_{rs}) *just above the sea surface* (denoted by z=0+, where z represents a depth) is obtained in prior to its implementation.

The R_{rs} for a wavelength λ is defined by

$$R_{rs}(\theta_v, \varphi_v, z=0+, \theta_s, \varphi_s, \lambda) \equiv L_w(\theta_v, \varphi_v, z=0+, \theta_s, \varphi_s, \lambda) / E_d(z=0+, \theta_s, \varphi_s,\lambda) \quad (1)$$

where L_w and E_d are the radiance and the downward plane irradiance at the observation angle (zenith angle θ_v, azimuth angle, φ_v) and the solar angle (zenith angle θ_s, azimuth angle φ_s). Morel and Gentili (2002) showed in their Eq. 9 that the Eq. (1) can be related to the absorption coefficient a_t and the backscattering coefficient of the bulk water b_{bt} by

$$R_{rs}(\theta_v,\varphi_v,z=0+,\theta_s,\varphi_s,\lambda)= R_g (W, z=0,\theta_s, \varphi_s, \lambda) F(\theta_v, \varphi_v,z=0-,\theta_s,\varphi_s,\lambda) [b_{bt} (z=0-,\lambda)/a_t(z=0-,\lambda)] \quad (2)$$

where R_g is a transmittance term for the interface between the above and below sea surface and depends on the wind speed, W. For convenience, all dependencies of the variables on illumination and observation geometries, depth, and wavelength etc in Eq. 2 are omitted hereafter, unless otherwise specified. In addition, $R_g \cdot F$ will be denoted by F' so that Eq.2 is simplified by

$$R_{rs} = F' [b_{bt}/a_t]. \quad (3)$$

The absorption coefficient of the bulk seawater is decomposed into the absorption coefficients of the pure seawater (a_w) and any other materials (a_t),

$$a=a_w+a_t. \quad (4)$$

Similarly, the backscattering coefficient of the bulk seawater is decomposed into the backscattering coefficients of the pure seawater (b_{bw}) and any other particles (b_{bp})

$$b_{bt}=b_{bw}+b_{bp}. \quad (5)$$

In the following sections, an algorithm to retrieve the absorption (a_t) and backscattering coefficients (b_{bp}) (and their components thereafter) will be described.

2. IOP algorithm

2.1 Derivation of the a_t and b_{bp}

Substitutions of Eqs. 4 and 5 into Eq. 3 give a set of equations for wavelengths λ_1 and λ_2:

$$\begin{aligned} R_{rs}(\lambda_1)\, a_0(\lambda_1) - F'(\lambda_1)\, b_{bp}(\lambda_1) &= F'(\lambda_1)\, b_{bw}(\lambda_1) - R_{rs}(\lambda_1)\, a_w(\lambda_1) \\ R_{rs}(\lambda_2)\, a_0(\lambda_2) - F'(\lambda_2)\, b_{bp}(\lambda_2) &= F'(\lambda_2)\, b_{bw}(\lambda_2) - R_{rs}(\lambda_2)\, a_w(\lambda_2), \end{aligned} \quad (6)$$

where R_{rs} is obtained by satellite observation and a_w and b_{bw} are assumed known for each λ (i.e. they are given by Morel, 1974; Pope and Fry, 1997 for example, although their values of a_w and b_{bw} may be corrected for temperature and salinity dependencies). Eq. 6 can be solved to derive a_t (λ_1 and λ_2) and b_{bp} (λ_1 and λ_2), when (1) the wavelength dependencies of the inherent optical properties (b_{bp} and a_t) and (2) $F'(\lambda)$ are known.

2.2 The wavelength dependencies of the inherent optical properties

The wavelength dependency of b_{bp} (denoted by ε_{bb}) may be modeled by

$$\varepsilon_{bb} = b_{bp}(\lambda_1) / b_{bp}(\lambda_2) = (\lambda_1/\lambda_2)^{-m} \quad (7)$$

where m is related to the particle size distribution and is set as a pre-defined parameter value in the present algorithm. The wavelength dependency of a_0 is expressed by

$$\varepsilon_a = a_t(\lambda_1) / a_t(\lambda_2), \quad (8)$$

and it is another algorithm parameter value pre-defined. According to in situ observation, $\varepsilon_a = a_t(\lambda=490\text{nm}) / a_t(\lambda=510\text{nm})$ is least variable and therefore applicable for a wide range of seawaters (Fig. 1, see Smyth et al., 2006). Since SGLI does not have 510nm, it is replaced by the 530nm. Substituting Eqs. 7 and 8 into Eq. 6, as well as a use of $R_{rs}(\lambda=490)$ and $R_{rs}(\lambda=530)$ observed by the satellite, gives

a_t (490), a_t (530), b_{bp}(490) and b_{bp}(530) for a known F' (Determination of F' will be described in the next subsection). Once b_{bp}(490) (or b_{bp}(530)) are obtained, substituting them into Eq. 7 gives b_{bp} at any wavelength λ for an "m" assumed: (e.g.)

$$b_{bp}(\lambda) = b_{bp}(490)\,(\lambda/490)^{m}. \quad (9)$$

When F' is known, Eq. 9 allows us to derive a_t at any SGLI short wavelength λ, using Eqs. 3-5:

$$a_0(\lambda) = F'(\lambda)\,[\,b_{bw}(\lambda) + b_{bp}(\lambda)\,] - a_w(\lambda). \quad (10)$$

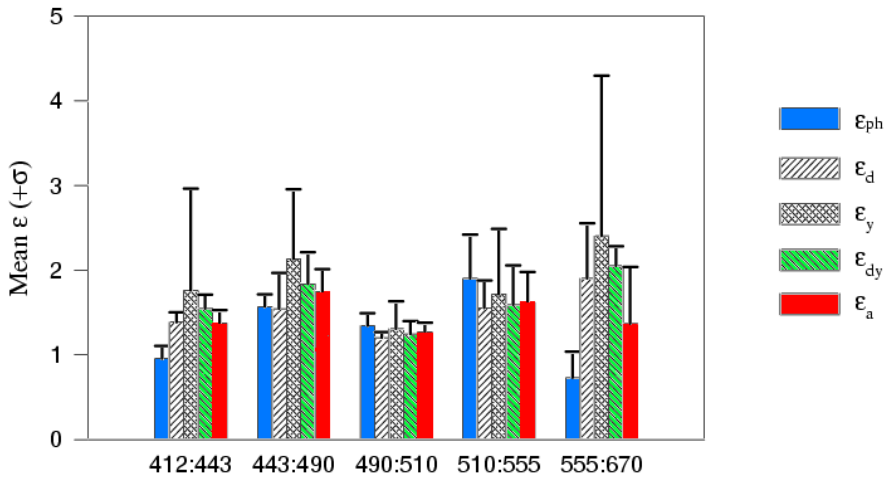

Fig. 1 Wavelength dependencies of the absorption coefficient of optical components determined from in situ observation (Smyth et al., 2006). ε_{ph}: phytoplankton absorption, ε_d: non-algal particle (NAP) absorption, ε_y: CDOM, ε_{dy}: NAP plus CDOM, ε_a: total absorption without pure sea water component.

2.3 Derivation of F'

Figure 2 shows a summary of derivation of F' (and a_t and b_{bp}). F' is initially assumed to be a certain value. Using the initial value, Equation 6 is solved to produce initial outputs of a_t and b_{bt}. These outputs are then used to search for the new value of F' from a forward radiative transfer simulation. However, to save a computation time for this simulation, the simulations for the various conditions of observation geometry (θ_v, φ_v), solar geometry (θ_s, φ_s) and inherent optical properties at SGLI-wavelengths were conducted to generate a Look-Up Table (LUT) of F', in prior to the algorithm implementation. Using the new value of F' obtained from the LUT(or the simulation), Eq. 6 is again solved to produce another set of a_t (λ) and b_t (λ)(i.e. second estimates), which are then used to search for a third, forth, … n^{th} estimation of F' (λ) using the same LUT. This procedure is repeated until a

convergence of $a_t(\lambda)$ and $b_t(\lambda)$ is reached. Also, when a pre-fixed number of iteration is implemented, the iteration is terminated. A value of F' (λ) at the convergence or termination is given as F' (λ) value to produce final outputs of a_t and b_{bp} using Eq. 6. The LUT is made as a function of θ_v, φ_v, z, θ_s, φ_s, a_t, b_t and λ. Note that, in the LUT, φ_v is defined such that a direction of wind is set to φ_v=0, which has π /2 phase difference with the solar principal plane.

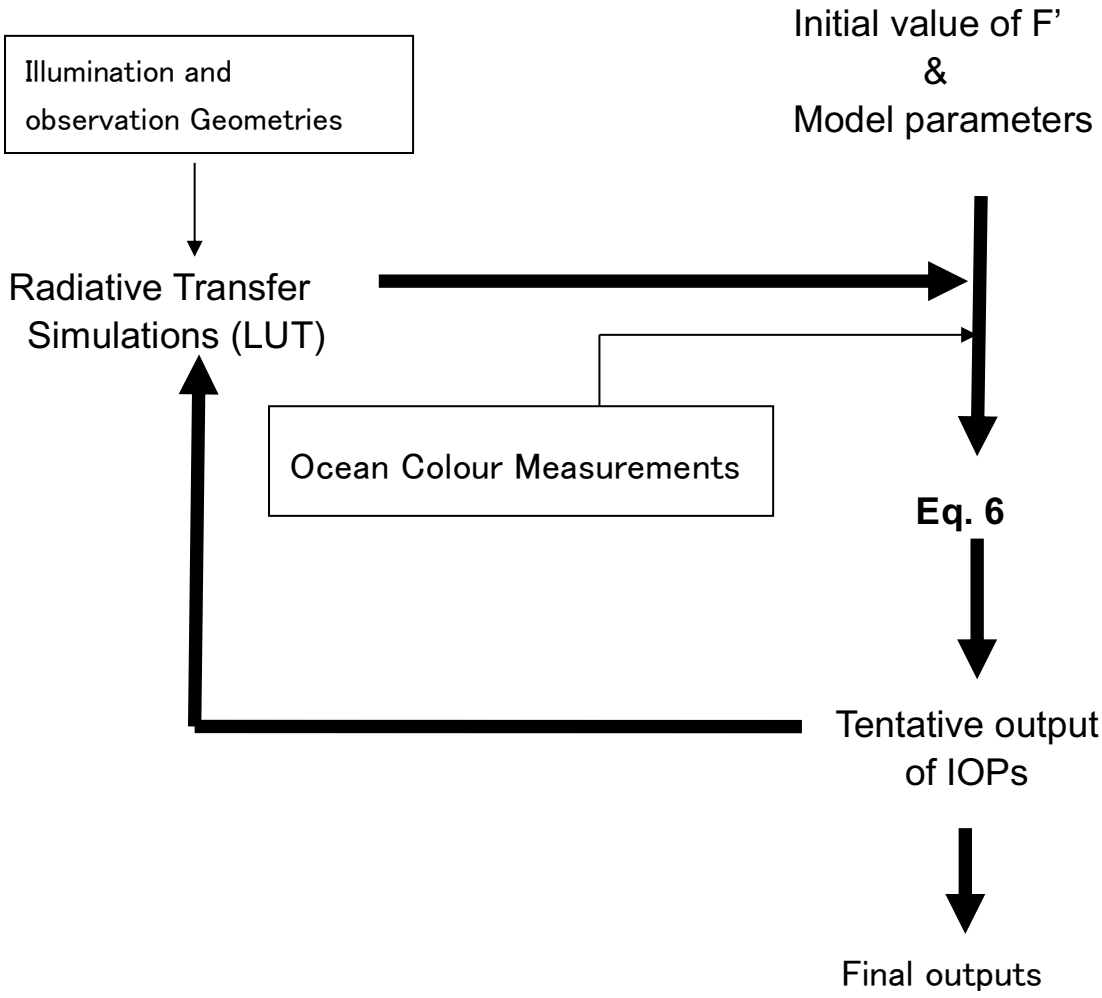

Fig. 2 Flow chart of the algorithm implementation

2.1 Decomposition of the IOPs of optical components from the IOPs of bulk seawater

The total absorption coefficient without pure seawater contribution a_t can further be decomposed by $a_t=a_{ph}+a_{dy}$ where the absorption coefficient of phytoplankton and of NAP plus chromophoric dissolved organic matters (CDOM) are denoted as a_{ph} and a_{dy}, respectively. The decomposition gives the simultaneous equations for two wavelengths λ_1 and λ_2.

$$a_o(\lambda_1)=a_{ph}(\lambda_1)+a_{dy}(\lambda_1)$$
$$a_o(\lambda_2)=a_{ph}(\lambda_2)+a_{dy}(\lambda_2). \quad (11)$$

In analogy to Eq. 6, Eq. 11 can be solved to obtain a_{ph} and a_{dy} at λ_1 and λ_2 when wavelength dependencies of a_{ph} and a_{dy} defined by $\varepsilon_{ph} = a_{ph}(\lambda_1) / a_{ph}(\lambda_2)$ and $\varepsilon_{ph} = a_{dy}(\lambda_1) / a_{dy}(\lambda_2)$ are known. Figure 1 shows that variations in ε_{ph} and ε_{dy} are least for the wavelength pair of λ_1=412nm and λ_2=443nm so that their values may be applied to a wide range of water types. Therefore, $\varepsilon_{ph}(412, 443)$ and $\varepsilon_{dy}(412, 443)$ are used in the present algorithm.

Using the modeled wavelength dependency of a_{dy}, or equivalently ε_{dy}, expressed by:

$$a_{dy}(\lambda)=a_{dy}(\lambda_1)\exp[-Y(\lambda-\lambda_1)], \quad (12)$$

a_{dy} for any SGLI short wavelength λ can be obtained using $a_{dy}(413)$ and $a_{dy}(443)$ derived as solution of Eq. 11.

Rearrangement of Eq. 11 gives

$$a_{ph}(\lambda)=a_0(\lambda) - a_{dy}(\lambda). \quad (13)$$

Since $a_0(\lambda)$ and $a_{dy}(\lambda)$ can be obtained for any SGLI short wavelength, Eq. 13 completes the derivations of a_0 , a_{ph}, a_{dy} and b_{bp} at the SGLI wavelengths. Note that a_t and b_{bt} can also be derived from these IOPs using Eqs. 4 and 5. Fig. 3 summarizes the sequence of the IOPs retrieval.

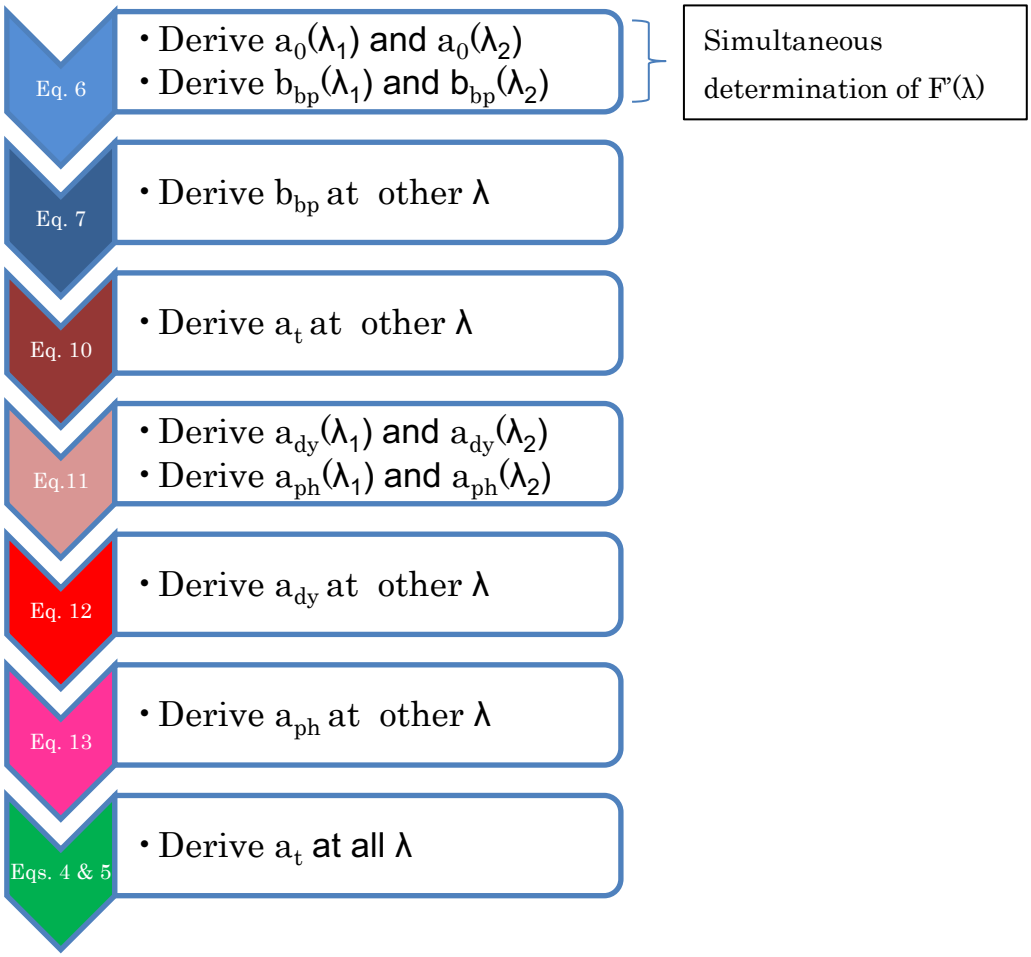

Fig. 3 Sequence of IOP retrieval.

3. Algorithm evaluation

Figs. 4-6 show examples of evaluation results of the IOP algorithm, using the NOMAD data set (Werdell and Bailey, 2005) from which simultaneous measurements of R_{rs} and IOPs can be obtained. The in situ R_{rs} is given as an input to the present IOP algorithm, and the algorithm outputs were compared to the in situ IOPs in the data set. Also Table 1-3 below summarizes statistical results of the evaluation.

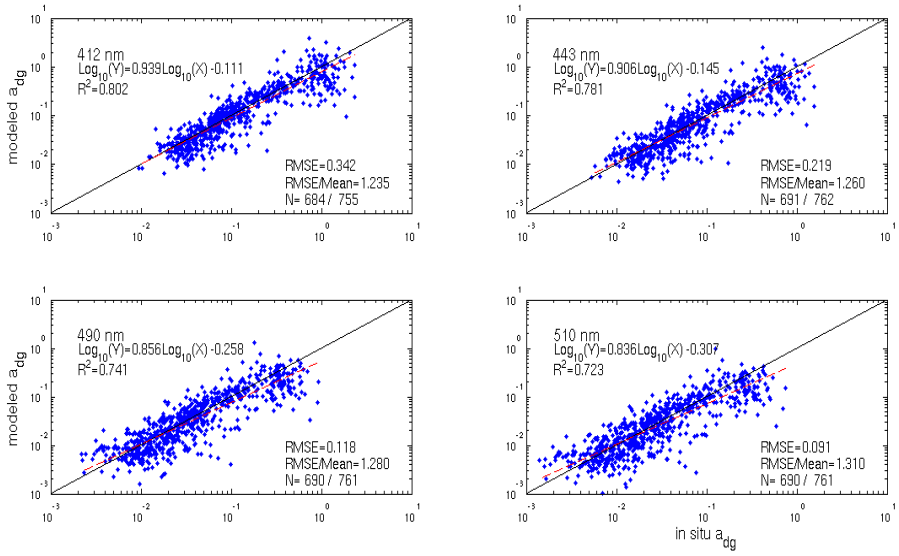

Fig. 4 Comparison between a_{dy} (a_{dg}) measured in situ and derived from the IOP algorithm.

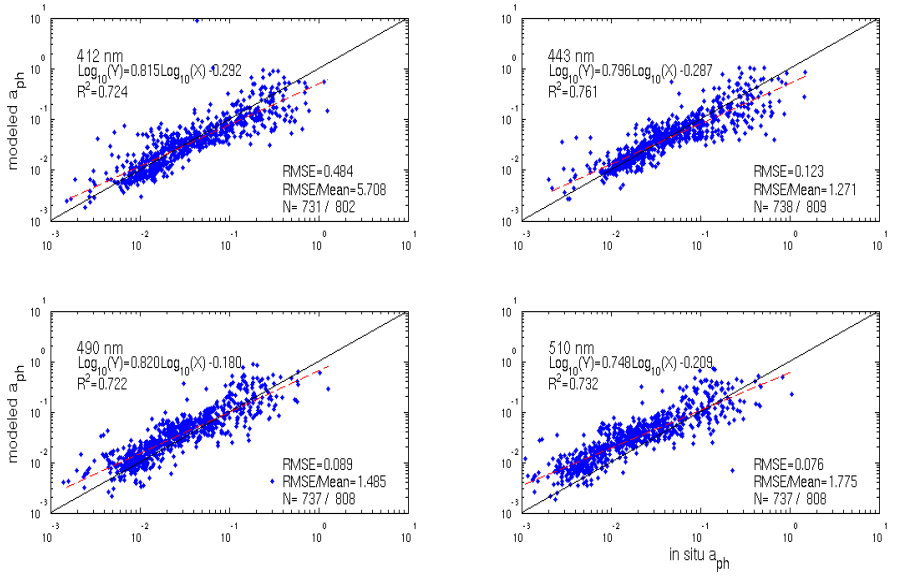

Fig. 5 Comparison between b_b measured in situ and derived from the IOP algorithm.

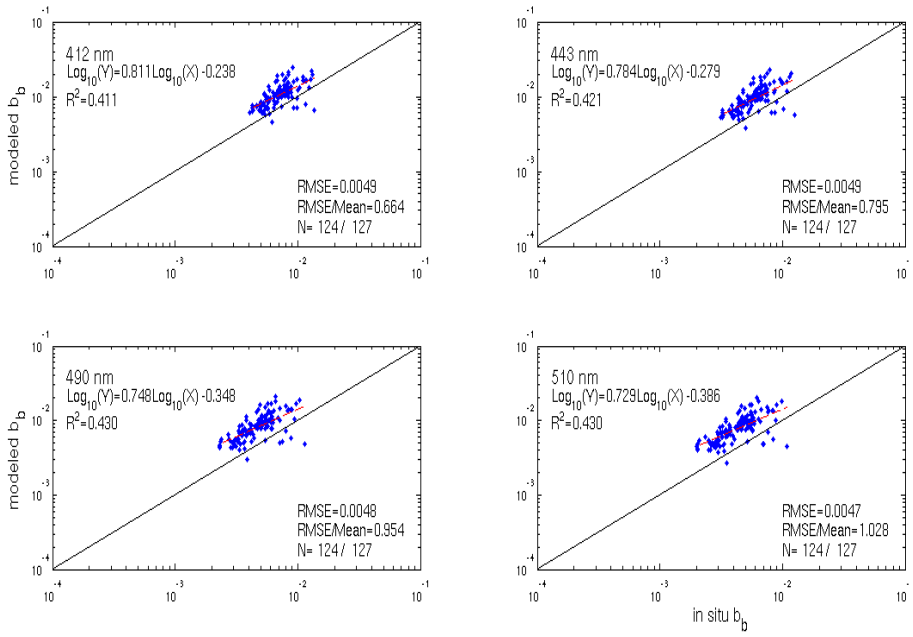

Fig. 6 Comparison between b_b measured in situ and derived from the IOP algorithm.

Table 1. Statistical results of algorithm evaluation for a_{dy} against in situ data

Wavelength#	slope#	intercept#	r^2#	RMSE*
412	0.939	-0.111	0.802	0.342
443	0.0.906	-0.145	0.781	0.219
490	0.856	-0.258	0.741	0.118
510	0.836	-0.307	0.723	0.091

#log scale, *Liner scale

Table 2. Statistical results of algorithm evaluation for a_{ph} against in situ data

Wavelength#	slope#	intercept#	r^2#	RMSE*
412	0.815	-0.292	0.724	0.484
443	0.796	-0.287	0.761	0.123
490	0.820	-0.180	0.722	0.089
510	0.748	-0.209	0.732	0.076

#log scale, *Liner scale

Table 3. Statistical results of algorithm evaluation for b_b against in situ data

Wavelength	slope#	intercept#	r^2#	RMSE*
412	0.811	-0.238	0.411	0.0049
443	0.784	-0.279	0.421	0.0049
490	0.748	-0.348	0.430	0.0048
510	0.729	-0.386	0.430	0.0047

#log scale, *Liner scale

References

Model A., D. Antoine and B. Gentili, Bidirectional reflectance of oceanic waters: accounting for Raman emission and varying particle scattering phase function, Appl. Opt., 41, 6289-6306, 2002.

Morel, A. and B. Gentili, Diffuse reflectance of oceanic waters III. Implication of bidirectionality for the remote-sensing problem, Appl. Opt., 35, 4860-4862, 1996.

Pope R. M. and E. S. Fry, Absorption spectrum (380-700nm) of pure water. II. Integrating cavity measurements, Appl. Opt., 36, 8710-8722, 1997.

Morel,A., Optical properties of pure seawater, in Optical Aspects of Oceanography, N. G. Jerlov and E. Steemann Nielson, ed., Academic Press, pp. 1-24, 1974.

Smyth, T.J., G. F. Moore, T. Hirata, J. Aiken, Semianalytic model for the derivation of ocean color inherent optical properties: description, implementation, and performance assessment, Appl. Opt., 45, 8116-8131, 2006.

Werdell, P. J. and S. W. Bailey, An improved in situ data set for bio-optical algorithm development and ocean color satellite validation, Remote Sens. Environ., 98, 122-140, 2005